NMR Evidence for Gapped Spin Excitations in Metallic Carbon Nanotubes

P. M. Singer,[1] P. Wzietek,[1] H. Alloul,[1] F. Simon,[2] and H. Kuzmany[2]
[1]*Laboratoire de Physique des Solides, UMR 8502, Université Paris-Sud, 91405 Orsay, France*
[2]*Institut für Materialphysik, Universität Wien, Strudlhofgasse 4, A-1090 Wien, Austria*
(Received 11 August 2005; published 29 November 2005)

We report on the spin dynamics of ^{13}C isotope enriched inner walls in double-wall carbon nanotubes using ^{13}C nuclear magnetic resonance. Contrary to expectations, we find that our data set implies that the spin-lattice relaxation time (T_1) has the same temperature (T) and magnetic field (H) dependence for most of the inner-wall nanotubes detected by NMR. In the high-temperature regime ($T \gtrsim 150$ K), we find that the T and H dependence of $1/T_1T$ is consistent with a 1D metallic chain. For $T \lesssim 150$ K we find a significant increase in $1/T_1T$ with decreasing T, followed by a sharp drop below $\simeq 20$ K. The data clearly indicate the formation of a gap in the spin excitation spectrum, where the gap value $2\Delta \simeq 40$ K ($\equiv 3.7$ meV) is H independent.

DOI: 10.1103/PhysRevLett.95.236403 PACS numbers: 71.20.Tx, 61.46.+w, 73.22.−f, 76.60.−k

The electronic properties of carbon nanotubes have been of a topic of intense investigation ever since their discovery in the early 1990s. According to band-structure calculations, the basic electronic structure of single-wall carbon nanotubes (SWCNT) is expected to depend on the chiral wrapping vector (n, m) across the graphene plane, where tubes for which $(2n + m)/3 =$ integer are metallic, while all other tubes are semiconducting [1–4] with a large $\sim$1 eV gap [5]. While STM and transport measurements on *isolated* tubes demonstrate the diversity of tube properties, significant measurements on *macroscopic* amounts of tubes are only possible in selected cases. Photoemission spectroscopy (PES) measurements on metallic tubes in bundles [6,7] suggest that strong electron-electron correlations can lead to a Tomonaga-Luttinger-liquid (TLL) state. Recently, double-wall carbon nanotubes (DWCNT) have been synthesized by filling SWCNT with fullerenes (so-called ''peapods'' [8]) followed by a high-temperature reaction which merges the fullerenes into inner tubes [9,10]. These DWCNT have some exceptional properties since the inner tubes are accommodated in a highly shielded environment under clean room conditions [11]. Raman experiments performed even on bucky paper material allows one to detect some significant properties of these inner tubes due to their small diameter (high curvature).

Nuclear magnetic resonance (NMR) is usually an excellent technique for probing the electronic properties at the Fermi level of metallic systems; take for instance conducting polymers, fullerenes, and high-temperature superconductors to mention a few. However the 1.1% natural abundance of ^{13}C with nuclear spin $I = 1/2$ limits the sensitivity of such experiments. Data taken on SWCNT essentially evidence a large distribution of properties since samples of identical tubes are presently out of reach. In this Letter, selective enrichment of the inner shells using ^{13}C isotope enriched fullerenes [12,13] in the peapod synthesis route is used to probe the specific properties of the inner tubes. The ^{13}C enrichment allows us to increase the ^{13}C NMR sensitivity by 2 orders of magnitude, and furthermore achieve *selective* ^{13}C enrichment of the inner shells alone. This provides us with the possibility of singling out the electronic properties of these inner tubes for the first time. We show that, although these tubes are distributed in diameter and chirality, their electronic properties display a strikingly homogeneous behavior. The magnetic properties of these inner-wall nanotubes behave as for a 1D metal at room T, but exhibit a pronounced gap below $\simeq 20$ K. This unexpected result reveals that this specific macroscopic collection of carbon nanotubes is an object displaying original physical properties worth studying in more detail with macroscopic experimental techniques.

All ^{13}C NMR data in this Letter were taken with the sample sealed in a 6 mm diameter glass tube filled with 200 mbar of high purity helium gas. Details of the synthesis techniques and various independent experimental evidences for the formation of 89% ^{13}C isotope enriched inner walls inside natural 1.1% ^{13}C enriched outer walls are reported elsewhere [12]. We probed the low frequency spin dynamics (or low energy spin excitations, equivalently) of the inner tubes using the spin-lattice relaxation time, T_1, defined as the characteristic time it takes the ^{13}C nuclear magnetization to recover after saturation. The signal intensity after saturation $S(t)$ was deduced by integrating the fast Fourier transform of half the spin echo for different delay times t. All data were taken with excitation pulse lengths $\pi/2 = 3.0$ μs and short pulse separation times of $\tau = 15$ μs [14]. We obtained the value of T_1 by fitting the t dependence of $S(t)$ to the form $S(t) = S_a - S_bM(t)$, where $S_a \simeq S_b$ (> 0) are arbitrary signal amplitudes, and

$$M(t) = \exp[-(t/T_1^e)^\beta] \quad (1)$$

is the reduced magnetization recovery of the ^{13}C nuclear spins. Figure 1 shows the results of $M(t)$ for the inner tubes as a function of the scaled delay time t/T_1^e, under various

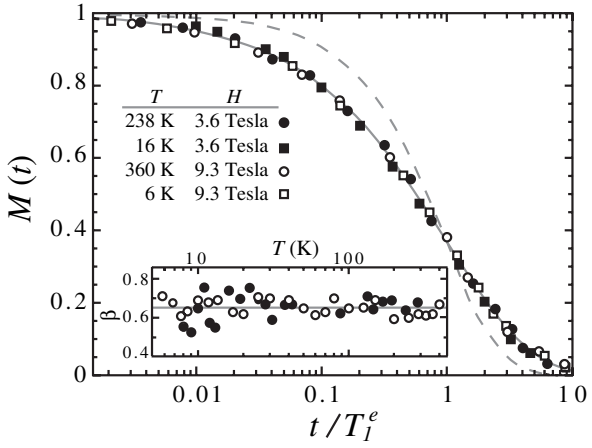

FIG. 1. Reduced nuclear magnetization recovery, $M(t)$, as a function of the scaled delay time t/T_1^e [see Eq. (1)], under various experimental conditions. Both axes are dimensionless. Solid gray curve shows stretched exponential fit with $\beta = 0.65$, while gray dashed curve shows single exponential with $\beta = 1$. Inset shows temperature dependence of the best fit values of β at 3.6 (●) and 9.3 T (○), and average value of the data set $\beta = 0.65$ (solid line).

experimental conditions listed. We find that $M(t)$ does not follow the single exponential form with $\beta = 1$ (dashed line), but instead fits well to the stretched exponential form with $\beta \simeq 0.65(5)$, which implies a distribution in underlying relaxation times T_1 across the sample. In such cases, T_1^e in Eq. (1) is directly proportional to the mean value $\bar{T}_1$ of the T_1 distribution as such $T_1^e = \bar{T}_1\beta/\Gamma(1/\beta)$, where Γ is the gamma function. We display the data in Fig. 1 on a semilog scale for the time axis in order to accentuate the data for earlier decay times and to illustrate the collapse of the data set for the upper 90% of the NMR signal. We find that the upper 90% of the $M(t)$ data is consistent with constant $\beta \simeq 0.65(5)$ (see inset), implying a constant underlying distribution in T_1 over a large range of experimental conditions. The lower 10% of the $M(t)$ data (corresponding to longer delay times) comes from the nonenriched outer walls which, as a result of their larger diameters, have much longer relaxation times under similar experimental conditions [15–18].

Two distinct origins for the multiexponential magnetization recovery can be considered. The first is due to the powder average over the spatial anisotropy in T_1. The distribution is independent of the tube properties, and can also be found in the ^{13}C NMR data for alkali doped fullerenes A_nC_{60} [19,20]. Given the similar diameter of C_{60} ($d = 0.71$ nm) to the average inner-wall diameter ($\bar{d} = 0.7$ nm [12,13]) in this Letter, we can expect comparable bonding effects for the electron orbitals. It has been shown that in A_nC_{60} the T_1 for ^{13}C is dominated by the dipole-dipole interaction between the electron spin in the $pp\pi$ bond and the ^{13}C nuclear spin [21]. In this case, the relaxation depends on the orientation of the p_π orbital (which is perpendicular to the tube surface) and the external magnetic field, and therefore contributes to the multiexponential form of the magnetization recovery for a powder average. This resultant T_1 distribution is independent of T and H.

Another source of multiexponential recovery is from a distribution of the inner tube properties themselves, such as their diameter. According to Raman scattering, the inner tubes have a mean diameter of $\bar{d} \simeq 0.7$ nm with a standard deviation of $\sigma \simeq 0.1$ nm [12,13]. Within this distribution lies a variety of tubes with different chirality and one can *a priori* expect to find metallic as well as semiconducting tubes [3]. If both semiconducting and metallic inner tubes existed in our sample, one would expect the ratio of the T_1's between the different tubes to increase exponentially with decreasing T below the semiconducting gap ($\sim$5000 K [5]), which would drastically change the underlying T_1 distribution with decreasing T. This change would manifest itself as a large change in the shape of the recovery $M(t)$, however, as shown in Fig. 1 this is not the case. We can therefore rule out the possibility of two components in T_1 with different T dependences, and instead we conclude that all T_1 components exhibit the same T and H dependence within experimental scattering.

The T_1 distribution in the sample, whether it arises from anisotropy or diameter distributions (or both), shows a uniform T and H dependence. It is therefore appropriate to follow the T and H dependence of the bulk value of the distribution [T_1^e in Eq. (1)], and thereby get insight into the homogenous electronic state of the inner tubes. In order to avoid unnecessary experimental scattering in T_1^e, we then go back and fit all the $M(t)$ data to Eq. (1) using a fixed value of $\beta = 0.65$. We plot the resulting temperature dependence of $1/T_1^eT$ in Fig. 2 for two different values of the magnetic field H. We can immediately separate the data

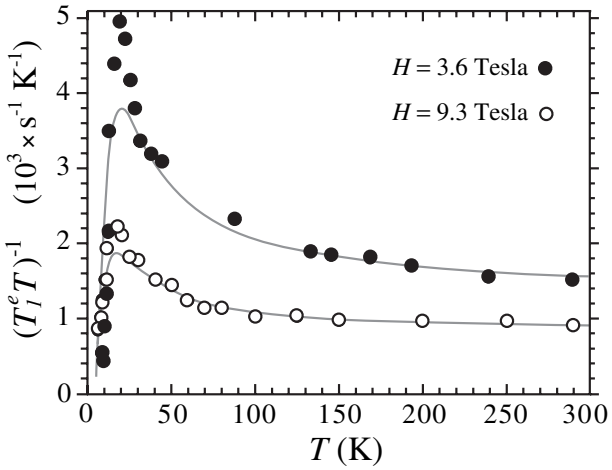

FIG. 2. Temperature dependence of spin-lattice relaxation rate divided by temperature, $1/T_1^eT$, in units of $(10^3 \times s^{-1}\,K^{-1})$. Gray curves are best fits to Eq. (4) with $2\Delta = 46.8(40.2)$ K for $H = 3.6(9.3)$ T, respectively.

into two temperature regimes; the high-temperature regime $\gtrsim 150$ K, and the low T regime $\lesssim 150$ K. At high temperatures we find that $1/T_1^eT$ is independent of T which indicates a metallic state [14], which given the arguments above, implies that all of the inner tubes are metallic. We also find a strong field dependence for T_1 which is best illustrated by plotting the high-temperature value of $1/T_1^eT$ against $1/\sqrt{H}$ for H values ranging from 1.2 to 9.3 T, as shown in Fig. 3. We find that the data fit well to the form

$$\frac{1}{T_1^eT} = A + B\frac{1}{\sqrt{H}}, \tag{2}$$

where A and B are constants, which is very suggestive of a 1D spin-diffusion mechanism for T_1 [22–24]. $B/\sqrt{H}$ corresponds to the diffusive contribution to the relaxation originating from the long wavelength (i.e., $q \simeq 0$) modes, while A corresponds to the nondiffusive contributions from $q > 0$ modes. A cutoff to the divergence in Eq. (2) as $H \rightarrow 0$ is often encountered in 1D spin chain systems [22–24] due to interchain coupling. In the present case, we can postulate that electron tunneling between inner to outer walls could cause similar cutoff effects, however the data down to the lowest field of $H = 1.2$ T indicate that the cutoff has not been reached yet. We therefore conclude that the high-temperature regime is consistent with a 1D metallic chain.

The origin of the unusual T dependence of $1/T_1^eT$ in the low temperature regime ($\lesssim$150 K) is not immediately obvious. We can, however, rule out certain possibilities. First, we can rule out the possibility of an activation type mechanism where T_1 is dominated by fluctuating hyperfine fields which are slowing down with decreasing T. If this were the case, the temperature where $1/T_1^eT$ reached its maximum would shift with the resonance frequency ω [14], or the applied magnetic field $\omega = \gamma_n H$ ($\gamma_n/2\pi =$ 10.705 MHz/T is the gyromagnetic ratio for ^{13}C), equivalently. As shown in Fig. 2, however, we find no evidence

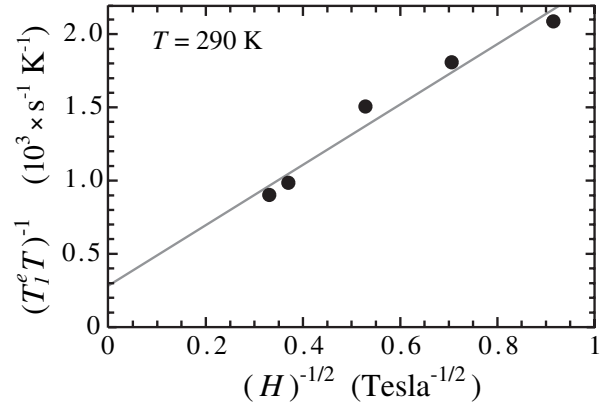

FIG. 3. $1/T_1^eT$, in units of $(10^3 \times s^{-1} K^{-1})$, at fixed $T =$ 290 K, plotted as a function of $1/\sqrt{H}$, in units of $(T^{-1/2})$. Linear fit corresponds to $1/T_1^eT = A + B/\sqrt{H}$ with $B =$ 0.00206 ($T^{1/2}$ s^{-1} K^{-1}) and $A = 0.00028$ (s^{-1} K^{-1}).

for a shift in the peak temperature with H. Furthermore, at low temperatures $1/T_1^eT$ is found to drop below its high-temperature value, which rules out the possibility of an activation contribution plus a T independent contribution. Second, we also rule out the possibility that the T dependence of $1/T_1^eT$ is a result of paramagnetic centers which can arise from wall defects or impurity spins. The fact that a pronounced gap exists in $1/T_1^eT$ implies a pronounced gap in the low energy spin excitation spectrum, which cannot be explained by the presence of paramagnetic centers. We note that at the lowest temperatures <5 K (not shown), T_1^e becomes so long (>300 s) that the low energy spin excitations specific to the homogeneous properties of the inner tubes become inefficient, and other excitations take over, possibly defect related. In such cases we find that the shape of $M(t)$ is no longer universal and that the underlying distribution in T_1 is smoothed out, possibly as a result of nuclear spin diffusion.

Having ruled out the above possibilities, we are then lead to consider the simplest explanation for the experimental data using a noninteracting electron model of a 1D semiconductor with a small secondary gap (SG). The SG may be a result of the finite inner-wall curvature [4,5,25,26], or perhaps the applied magnetic field itself [27]. We can fit the $1/T_1^eT$ data using this noninteracting model with only one free parameter, the homogeneous SG, 2Δ. We start by taking the normalized form of the gapped 1D density of states $n(E)$ [5]

$$n(E) = \begin{cases} \frac{E}{\sqrt{E^2-\Delta^2}} & \text{for} \quad |E| > \Delta \\ 0 & \text{otherwise} \end{cases} \tag{3}$$

also known as a van Hove singularity (E is taken with respect to the Fermi energy). We then use Eq. (3) to calculate $1/T_1^eT$ [28] as such:

$$\frac{1}{T_1^eT} = \alpha(\omega)\int_{-\infty}^{\infty} n(E)n(E+\omega)\left(-\frac{\delta f}{\delta E}\right)dE, \tag{4}$$

where E and ω are in temperature units for clarity, f is the Fermi function $f = [\exp(E/T) + 1]^{-1}$, and the amplitude factor $\alpha(\omega) = A + B'/\sqrt{\omega}$ is taken directly from Eq. (2) and Fig. 3 (where $B' = 4.53 \times 10^{-5}$ s^{-1} $K^{-1/2}$ for $\omega \equiv H$ in temperature units). We note that factoring out the diffusion effects from the integral in Eq. (4) is an approximation valid only if A and B are T independent. Equation (4) cannot be solved analytically, therefore we resort to numerical integration. The results of the best fit to Eq. (4) are presented in Fig. 2, where $2\Delta = 43(3)$ K ($\equiv$3.7 meV) is found to be H independent (within experimental scattering) between 9.3 and 3.6 T. We note that at the largest external field of 9.3 T, $\omega = 4.5$ mK $\ll \Delta, T$, however, ω must be retained inside the integral. This is a consequence of the one dimensionality which yields a logarithmic divergence inside the integral of the form $\ln(T/\omega)$ for $T \lesssim \Delta$.

What could possibly be the origin of the observed gap?—Tight binding calculations predict that applied magnetic fields can induce SG's of similar magnitude for metallic SWCNT [27]. However, such a scenario is excluded here from the absence of field dependence of the observed gap. Our data would be more consistent with a curvature induced SG for metallic tubes [4,5,25,26], however, for our typical inner tubes the predicted values, $\sim$100 meV, are over an order of magnitude larger than our experimental data. Other scenarios, such as quantization of levels due to finite short lengths of the nanotubes could be considered as well; however, in all these cases a behavior independent of tube size and chirality is certainly not expected.

This leads us to consider the effects of interactions in a 1D metallic system. According to TLL theory, electron-electron interactions lead to an increase in $1/T_1T$ by a power law with decreasing T [29], which is a direct consequence of the 1D electronic state. It is also known that 1D metallic systems possess a Peierls instability due to electron-phonon interactions. At half filling the instability causes a bond alternation with the opening of a small collective gap [3], which could explain the sharp drop in $1/T_1T$ below $\simeq 20$ K. This scenario may account for the data, although here again, the independence on tube geometry should be accounted for.

In conclusion, we have shown that the T_1 recovery data indicate that most of the inner tubes have similar T and H dependences, with no indication of a metallic/semiconductor separation due to chirality distributions. At high temperatures ($T \gtrsim 150$ K) $1/T_1^eT$ of the inner tubes exhibit a metallic 1D spin-diffusion state, with no low-field cutoff down to 1.2 T. This metallicity could result from charge transfer from the outer to the inner tubes, however this speculation ought to be confirmed by independent experiments and theoretical calculations. Below $\sim$150 K, $1/T_1^eT$ increases dramatically with decreasing T, and a gap in the spin excitation spectrum is found below $\simeq 20$ K. We list various interpretations for this temperature dependence, ranging from a noninteracting secondary band-gap model, to a 1D interacting electron model with a small collective gap. First, these results should stimulate further experimental investigations on diversely synthesized DWCNT in order to check whether these observations are specific to the peapod synthesis route. Second, theoretical work on the incidence of 1D interactions for inner-wall nanotubes inside DWCNT should be helpful in sorting out the origin of our astonishing experimental evidence.

Support from the EU Projects No. HPMF-CT-2002-02124, No. BIN2-2001-00580, and No. MEIF-CT-2003-501099, and the Austrian Science Funds (FWF) Project No. 17345, and the Magyary programme, are recognized. The authors also wish to thank V. Zólyomi and J. Kürti for valuable discussions.

[1] J. W. Mintmire *et al.*, Phys. Rev. Lett. **68**, 631 (1992).
[2] R. Saito *et al.*, Phys. Rev. B **46**, 1804 (1992).
[3] R. Saito, G. Dresselhaus, and M. Dresselhaus, *Physical Properties of Carbon Nanotubes* (Imperial College Press, London, 1998).
[4] N. Hamada *et al.*, Phys. Rev. Lett. **68**, 1579 (1992).
[5] J. W. Mintmire and C. T. White, Phys. Rev. Lett. **81**, 2506 (1998).
[6] H. Ishii *et al.*, Nature (London) **426**, 540 (2003).
[7] H. Rauf *et al.*, Phys. Rev. Lett. **93**, 096805 (2004).
[8] B. W. Smith *et al.*, Nature (London) **396**, 323 (1998).
[9] B. W. Smith and D. E. Luzzi, Chem. Phys. Lett. **321**, 169 (2000).
[10] S. Bandow *et al.*, Chem. Phys. Lett. **384**, 320 (2004).
[11] R. Pfeiffer *et al.*, Phys. Rev. Lett. **90**, 225501 (2003).
[12] F. Simon *et al.*, Phys. Rev. Lett. **95**, 017401 (2005).
[13] F. Simon *et al.*, Phys. Rev. B **71**, 165439 (2005).
[14] C. P. Slichter, *Principles of Magnetic Resonance* (Springer-Verlag, New York, 1989), 3rd ed.
[15] X.-P. Tang *et al.*, Science **288**, 492 (2000).
[16] C. Goze-Bac *et al.*, Carbon **40**, 1825 (2002).
[17] H. Shimoda *et al.*, Phys. Rev. Lett. **88**, 015502 (2002).
[18] A. Kleinhammes *et al.*, Phys. Rev. B **68**, 075418 (2003).
[19] R. Tycko *et al.*, Phys. Rev. Lett. **68**, 1912 (1992).
[20] V. Brouet *et al.*, Phys. Rev. B **66**, 155122 (2002).
[21] V. Antropov *et al.*, Phys. Rev. B **47**, R12 373 (1993).
[22] J.-P. Boucher *et al.*, Phys. Rev. B **13**, 4098 (1976).
[23] G. Soda *et al.*, J. Phys. (Paris) **38**, 931 (1977).
[24] C. Bourbonnais *et al.*, Phys. Rev. B **44**, 641 (1991).
[25] C. L. Kane and E. J. Mele, Phys. Rev. Lett. **78**, 1932 (1997).
[26] V. Zólyomi and J. Kürti, Phys. Rev. B **70**, 085403 (2004).
[27] J. P. Lu, Phys. Rev. Lett. **74**, 1123 (1995).
[28] T. Moriya, J. Phys. Soc. Jpn. **18**, 516 (1963).
[29] H. Yoshioka, J. Phys. Chem. Solids **63**, 1281 (2002).